DOI 10.1007/s11141-024-10325-8
Radiophysics and Quantum Electronics, Vol. 66, No. 9, February, 2024
(Russian Original Vol. 66, No. 9, September, 2023)

MERGING AND STRIPPING REGIMES IN CLOSE PAIRS OF RELATIVISTIC STARS: PROSPECTS FOR MODELS OF SHORT GAMMA-RAY BURSTS

A. V. Yudin,[1] **S. I. Blinnikov,**[1,2,3,4] **N. I. Kramarev,**[1,3]
and M. Sh. Potashov[1,4] *

UDC 524.387

We consider the current status of the binary neutron star stripping model to explain short gamma-ray bursts. After the historical joint detection of the gravitational wave event GW170817 and accompanying gamma-ray burst GRB170817A, the production of short gamma-ray bursts in the neutron star coalescence has been reliably confirmed. Many properties of GRB170817A that turned out to be peculiar compared to other short gamma-ray bursts are naturally explained in the stripping model proposed in our works in 1984. We emphasize the role of D. K. Nadyozhin (1937–2020), who quantitatively predicted the GRB and kilonova properties back in 1990. We also discuss problems that need to be solved in the context of this model, especially in simulations using the smoothed-particle hydrodynamics method.

1. INTRODUCTION

Long gamma-ray bursts (GRBs) most likely occur during collapse of "hypernovae," which are a subgroup of type Ic supernovae [1–5]. These events can be explained by the rapid collapse of the core of a massive star into a black hole (with mass $M \sim 40M_{\odot}$, where $M_{\odot}$ is the mass of the Sun), which lost its outer hydrogen and helium shells. These supernovae are called hypernovae because they usually have a much higher kinetic energy of explosion than that of ordinary supernovae. Something fundamentally different was proposed for short GRBs long before the long GRB models appeared.

The first ideas about the merging of a neutron star (NS) and a black hole, related to short gamma-ray bursts, were put forward by Lattimer and Schramm [6,7] (they even discussed the r-process of nucleosynthesis within this hypothesis). Detailed scenario for the merging of two neutron stars was developed by Clark and Eardley [8], but not a word was said about GRB in their important paper. They discussed in detail not only merging, but also stripping of a low-mass neutron star.

What is the difference between merging and stripping mechanisms? Two neutron stars revolving around each other must come closer due to the loss of the angular momentum due to the radiation of gravitational waves. The merging mechanism is as follows. By getting closer at a sufficient distance, neutron stars in just the last few revolutions merge into a single object, namely, a black hole or, less likely, into a rapidly rotating neutron star. In this case, part of matter may be ejected from the system due to tidal interaction [9]. In addition, due to the extreme acceleration of the rotation of matter and its heating, a highly collimated ejection of matter (jet) may form. This pattern of neutron star coalescence is now generally accepted (see, for example, [10]), although many of its details remain unclear.

* marat.potashov@gmail.com

[1] National Research Center "Kurchatov Institute"; [2] N. L. Dukhov All-Russia Research Institute of Automation [3] P. K. Sternberg State Astonomical Institute of the M. V. Lomonosov Moscow State University; [4] M. V. Keldysh Institute of Applied Mathematics of the Russian Academy of Sciences, Moscow, Russia. Translated from Izvestiya Vysshikh Uchebnykh Zavedenii, Radiofizika, Vol. 66, No. 9, pp. 720–734, September 2023. Russian DOI: 10.52452/00213462_2023_66_09_720 Original article submitted April 18, 2023; accepted June 22, 2023.

The fundamental difference between the stripping mechanism and rapid merging is a long-term process (many revolutions of a binary system) by which one star flows into another. Note that a sufficient asymmetry in the masses of the components of a binary system is required to implement this scenario. As the NSs approach each other, the component that has the lower mass (we denote it M_2) fills its Roche lobe first because of having a larger radius, and starts to flow to a more massive companion (with mass M_1) through the internal Lagrange point. Asymmetry of the system increases and the companions move apart due to the approximate conservation of the angular momentum of the system. However, the flow does not stop (is stable) for two reasons: first, the loss of angular momentum due to the radiation of gravitational waves still moves the NSs closer to each other, and second, the radius of the NS of a lower mass starts to increase. The latter fact follows from the properties of the mass–radius ($M-R$) diagram of the NS [11].

As a result of the mass exchange, M_1 increases, but the radius of this component remains approximately constant or decreases, while M_2 decreases with increasing radius. When M_2 reaches a value corresponding to the minimum possible NS mass $M_{\min} \sim 0.1 M_{\odot}$, an explosion will occur, which, in fact, produces a gamma-ray burst.

As a result of accretion of companion matter, the remaining single, more massive NS can, in principle, either collapse into a black hole or leave the place of interaction with significant (up to 1000 km/s) speed.

This scenario was described in detail in a visionary article by [8], but without mentioning the gamma-ray burst accompanying the explosion of a low-mass NS. The first firm prediction about the birth of a gamma-ray burst in a binary system, and precisely in stripping regime, was done by S. I. Blinnikov with co-authors [12]. In the subsequent paper [13] with D. K. Nadyozhin, hydrodynamic modeling of the explosive destruction of a low-mass NS was performed and many properties of the accompanying short gamma-ray burst were predicted. Among other things, it was shown there that the entire explosion process takes about one-tenth of a second, the gamma-ray radiation being generated by a very low-mass outer NS matter layer accelerated to relativistic velocities due to the cumulation effect when the shock wave reaches the surface. Hydrodynamic modeling of this process within the framework of relativistic hydrodynamics was recently discussed in [14].

However, this stripping scenario was forgotten for many years, first, due to the low energy of the resulting GRB, and second, due to the lack of a generation mechanism of the accompanying jet (the explosion of a low-mass NS is almost spherically symmetrical, see [15]). In addition, there were serious doubts about the existence of the regime of stable flow of matter [16].

2. GRB170817A AND THE STRIPPING MODEL

On August 17, 2017, LIGO detectors (with the participation of Virgo) recorded a very long signal of gravitational waves (GWs) [17]. Unlike the previous ones, this event corresponded to masses of merging objects, characteristic of neutron stars, not black holes. 1.7 s after the peak of a GW signal, FERMI and INTEGRAL spacecraft detected a short gamma-ray burst GRB170817A [18], and another 11 hours later a kilonova was discovered [19] in the galaxy NGC4993, which is 40 Mpc away from the Earth. Already in 2023, it was shown [20] that this kilonova was spherical, in complete contradiction with jet models and in complete agreement with the stripping model.

This success of multi-channel astronomy is significant in that this gamma-ray burst turned out to be very peculiar. In particular, it was 10^4 times weaker than other well-known short gamma-ray bursts [18], was soft rather than hard, and showed no signs of a strong jet [21].

As we showed in [22], all the features of GRB170817A obtain a natural explanation in the stripping mechanism during the mass exchange of NSs. Let us trace the sequence of events following [23] and Fig. 1.

Thus, two NSs with masses $M_1 = 1.6 M_{\odot}$ and $M_2 = 1.15 M_{\odot}$ move closer because of the losses due to gravitational radiation, whose luminosity L_{GW} (Fig. 1c) is determined by the formula [24]

$$L_{\mathrm{GW}} = \frac{32}{5}\frac{G^4}{c^5}\frac{M_1^2 M_2^2 (M_1+M_2)}{a^5}, \tag{1}$$

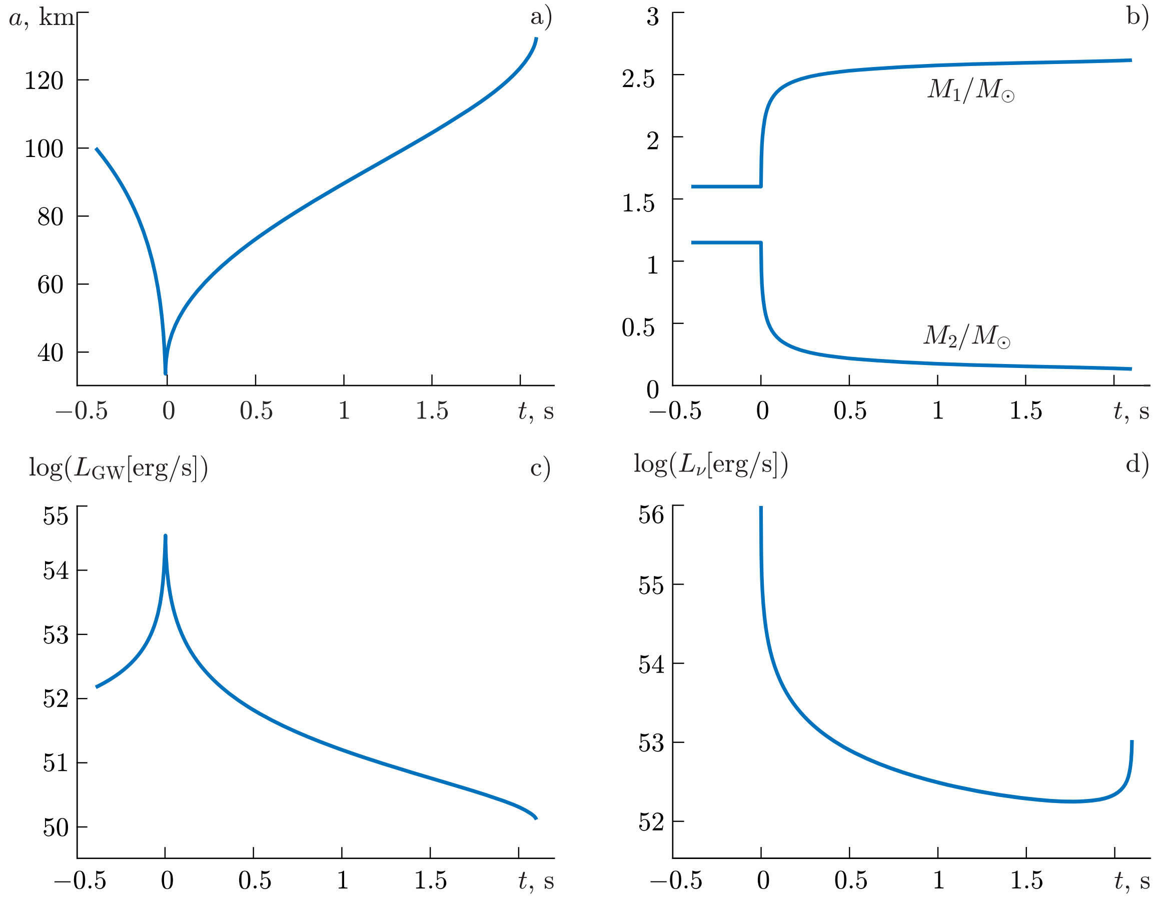

Fig. 1. Distance a between the components (a), their masses M_1 and M_2 (b), gravitational-wave L_{GW} (c), and "neutrino" L_ν (d) luminosities as functions of time t.

where G is the gravitational constant and c is the speed of light in empty space. When the distance a between NSs decreases to approximately 40 km, the less massive component M_2 fills its Roche lobe and starts to give its mass to the component M_1. The components move away from each other, which, together with an increase in mass asymmetry of the system, leads, according to Eq. (1), to a sharp drop in luminosity of gravitational radiation. In this case, M_2 matter accreting on the surface of M_1 leads to the release of energy with the power

$$L_\nu = \frac{GM_1\dot{M}_1}{R_1}, \tag{2}$$

where R_1 is the radius of the more massive NS, and the dot means differentiation with respect to time. Here, following [8], we attribute this energy release to the neutrino channel, although part of it will inevitably occur in the form of electromagnetic radiation. This radiation may be a precursor to the main gamma-ray burst about a second before the trigger (see, e, g., [25]). If the Eddington luminosity is exceeded (it is more than ten orders of magnitude less than the neutrino luminosity L_ν), the electromagnetic channel of energy release should lead to the formation of a dense shell of matter blown away by the radiation pressure. We plan to take this possibility into account in the future. For now, following Clark and Eardley [8], we consider only the simplest conservative case. The action of the accompanying effects related to non-conservative mass exchange on the evolution of the system will be discussed in subsequent works.

When the mass M_2 decreases to approximately $0.2M_\odot$, the flow stability is lost (see the criterion (4) in what follows) and the star rapidly, on a hydrodynamic time scale, reaches the minimum mass value M_{min} and explodes, producing a gamma-ray burst.

Thus, the most important parameter t_{str} appears in the stripping mechanism, namely, the time between the peak of the gravitational-wave signal and the gamma-ray burst. In the example considered, this parameter is slightly more than 2 s. Its value is determined by the equation of state BSk26 [26] used here, which satisfies modern constraints on NS parameters [27], and mass values consistent with LIGO—Virgo data on the signal source GW170817 [28]. It is striking that in the example discussed in [8], with the masses $M_1 = 1.3M_\odot$ and $M_2 = 0.8M_\odot$ and outdated equation of state, the authors obtained for $t_{\rm str}$ exactly the value 1.7 s!

In this paper, the problem of matter flow in a close binary system is solved initially in two ways in parallel. The first method is a semi-analytical approach that uses the approximation of point masses with spin. The second method is completely numerical and uses the method of smoothed-particle hydrodynamics.

3. MARGIN BETWEEN SCENARIOS AND THE FLOW STABILITY

What will happen for other values of the component masses, other things being equal? For the answer, we address Fig. 2, which shows the quantity $t_{\rm str}$ as a function of M_1 and M_2 for the region where the stripping mechanism is operative. Simulations were performed for the equation of state BSk26 [26]. The range of masses corresponding to the GW170817 signal [28] is also shown: the darker part of the curve corresponds to the case of low initial spins of the components, and the light part, to the case of high ones. The specific mass value we used to construct Fig. 1 is shown by a circle. It can be seen that for none of the M_1 and M_2 mass values does the value $t_{\rm str} = 1.7$ s exist. However, this is only a property of this particular equation of state we used. For other equations of state this is not the case, but, as we showed in [29,30], other factors, not taken into account in the above simple version of the stripping mechanism, are more important there.

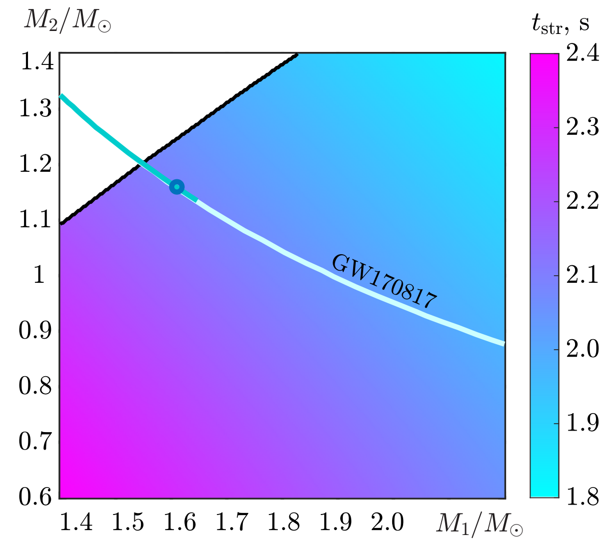

Fig. 2. The $t_{\rm str}$ value for different masses of the components of the binary system with the equation of state BSk26. The margin between scenarios (white color denotes merging and the shades of blue, stripping), the mass range dictated by GW170817, and specific values used to construct Fig. 1 (circled) are also shown.

Let us discuss the margin between the scenarios in Fig. 2. It was obtained from the following considerations: if a flow occurs, then the low-mass component M_2 of the binary system fills its Roche lobe. It was shown in [31] that even if the donor had a large intrinsic angular momentum before the flow started, this momentum is quickly lost during stripping. Therefore, we can assume that the low-mass component is in the co-rotation regime. From the above it follows that during the flow the radius R_2 of this component is equal to the size of the limiting Roche lobe $R_{\rm Roche}$, which is parameterized [32] as

$$R_{\rm Roche} = af(q), \tag{3}$$

where a is the distance between NSs and $f(q)$ is the known [33] function of the mass asymmetry parameter $q = M_2/(M_1+M_2)$. The flow stability parameter in this case can be written as [29,34]

$$\frac{{\rm d}(\ln R_2)}{{\rm d}(\ln M_2)} \geqslant \frac{{\rm d}[\ln f(q)]}{{\rm d}(\ln q)} - 2\frac{1-2q}{1-q}. \tag{4}$$

It is seen that the flow stability, besides q, is determined by the NS mass–radius dependence, or, which is the same, the equation of state. In the unshaded region in Fig. 2 the stable flow, according to criterion (4), is impossible and the merging scenario takes place.

Bringing a low-mass NS to the lower theoretical mass limit requires a stable regime of flow of matter.

Why there are no signs of stable flow of matter in the numerous three-dimensional simulations performed to study the NS merging process? This issue has been repeatedly explored in the literature, both analytically in the Newtonian approximation [16] and numerically [35,36], in the post-Newtonian approximation [37–39] and within the framework of the general theory of relativity [40]. These papers studied the problem of stability for various equations of state of neutron matter, as well as various factors $q' = M_2/M_1$. But even in the Newtonian approximation, with the same parameters of the problem, some researchers obtained a global dynamic instability, while others had a stable flow of matter over many revolutions of the binary system. Independent verification is required even in the classical approximation. This test was started in [29], but without taking into account gravitational radiation. Below we consider some of the research results on this issue.

4. STRIPPING OR MERGING: PHANTOM CODE SIMULATION

Modern three-dimensional simulations of the neutron star merging process are very complex and are expensive in terms of computer resources [41]. Therefore, the problem of choosing the initial simulation configuration and/or the initial point in time is extremely important. There is a temptation to save resources by skipping the "dull" part, namely, the actual process of NS coming closer (especially since the procedure for correctly taking into account gravitational radiation in a 3D problem is not at all simple [42]) and move immediately to a complex nonlinear merging process. It seems to us that this is at least part of the answer to the problem that this section is devoted to.

The process of stripping of outer layers, formation of a jet, and flow of matter from a low-mass NS to a massive component occurs at densities significantly lower than the densities in the depths of the NS, so when describing these processes there is no point in using exact equations of state for superdense neutron matter. Therefore, we use here simplified equations of state; see Eq. (5) below.

To perform 3D numerical experiments at this stage in order to clarify the problem of stability of the flow process, we chose the open PHANTOM code [43]. It is based on the method of smoothed particle hydrodynamics (Smoothed Particle Hydrodynamics, SPH). This is a Lagrangian gridless method for Newtonian dynamics and gravity. Particles in this method are bulk elements of the medium of unspecified shape, to which physical characteristics are assigned, including coordinates, speed, mass, density, typical sizes, temperature, pressure, and so on. PHANTOM has a constraint: all particles have the same mass. The discrete representation of the medium in the form of smoothed particles involves the replacement of continuous characteristics $f(r)$ into piecewise constant quantities f_i, determined for each particle i through the sum of N quantities f_j for the neighbor particles j lying around the particle i, using the weighting (smoothing) kernel function. Approximation of spatial derivatives on the right-hand sides of conservation law equations in SPH is carried out through the transfer of derivatives in the particle coordinate to the derivative of the smoothing kernel function. Based on solutions to the equations of motion, continuity, energy, and other, the particles change positions, density, and temperature, a new pressure field is calculated for them, and so on.

To model close binary systems, PHANTOM initially builds two stars with given masses and radii and with density profiles depending on the equation state of matter. To do this, stars are "assembled" from SPH particles and pass a relaxation procedure, during which the complete system of dynamic equations of motion of self-gravitating particles is solved. In PHANTOM, the unit of time is a dimensionless quantity

$$u_{\rm time} = \sqrt{\frac{u_{\rm dist}^3}{G u_{\rm mass}}}.$$

Here $u_{\rm dist}$ is the unit distance (kilometer) and $u_{\rm mass}$ is the unit mass ($M_\odot$). For the systems considered below, $u_{\rm time} \sim 3 \cdot 10^{-3}$ ms. The authors of the code recommend carrying out the relaxation procedure on times of the order of $10^2 u_{\rm time}$. The simulation is then restarted to model the behavior of the resulting equilibrium stars in orbit.

4.1. Equation of state and hydrodynamics

At this stage, we model the NS using a very simple equation of state that connects pressure P, density ρ, and temperature T:

$$P = K\rho^\gamma + \rho\frac{\mathcal{R}T}{\mu}. \tag{5}$$

Here, K is the polytropic coefficient, γ is taken equal to 2, $\mathcal{R}$ is the universal gas constant, and μ is the average molecular weight, which can be taken equal to 1 in the case of a NS. Equation (5) at $\gamma \sim 2$ approximately models the behavior of other, more physical equations of state (e. g., BSk26 [26]) for NS matter in the region of abrupt mass variation for an almost constant radius in the mass–radius diagram. We added Eq. (5) into the PHANTOM code.

The motion of SPH particles in the PHANTOM simulation is given by the equation

$$\frac{\mathrm{d}\mathbf{v}}{\mathrm{d}t} = -\frac{\nabla P}{\rho} + \Pi_{\text{shock}} + \mathbf{a}(\mathbf{r}, t), \tag{6}$$

and the internal energy, by the first law of thermodynamics,

$$\frac{\mathrm{d}E}{\mathrm{d}t} = -\frac{P}{\rho}(\nabla\cdot\mathbf{v}) + \Lambda_{\text{shock}}. \tag{7}$$

Here, $\mathbf{v}$ is the speed of the SPH particle, $\mathbf{a}(\mathbf{r}, t)$ is its acceleration at a point with radius vector $\mathbf{r}$ at the time t, caused by self-gravity or given external forces, E is the internal energy per unit mass, and the terms Π_{shock} and Λ_{shock} describe the motion and energy variation due to dissipation, which are necessary for correct allowance for entropy increase at the front of shock or acoustic waves. Unlike the grid methods, where the numerical viscosity appears in schemes in a natural way, in the SPH method, artificial viscosity terms should explicitly be added, since the numerical viscosity does not arise in it during the sampling because of the Hamiltonian nature of this method. Taking into account viscosity also prevents mutual penetration of particles into each other [43–45]. We use a description based on the concept of artificial viscosity (see [43, Eqs. (39) and (42)]). Allowance for Λ_{shock} in Eq. (7) and thermal part in Eq. (5) makes it possible to exclude non-physical oscillations of the star as a whole. In this case, such oscillations should be damped. In principle, in Eq. (5) one could use the true pressure versus temperature dependence in the equation of state of degenerate matter [46]. But in this case, the purpose of introducing this additive was only to "remove" acoustic mechanical oscillations of the star and pumping of their energy into the thermal part. Since the energy of this part is much less than the energy of degenerate matter, the form of the additive is not so important and we dwell on the simplest option.

In the SPH method, in the case of neglecting dissipation and external forces, the Hamiltonian of the system is preserved along the solution. For problems of motion along Kepler orbits, it is convenient to use symplectic, symmetric integration schemes (e. g., the Störmer–Verlet scheme of second-order accuracy), which preserve the Hamiltonian close to the true one along the approximate solution (the so-called constrained Hamiltonian). However, when taking into account dissipative terms and the work of external forces, the Hamiltonian will no longer be preserved, the system itself will cease to be Hamiltonian, and the acceleration of particles will depend on their speed. In PHANTOM, for this case, a modification of the Störmer–Verlet scheme is used, in which iterations are added to correctly solve the implicit numerical scheme with the dependence of acceleration on speed. To take into account external forces in PHANTOM, additional iterative substeps are added into the scheme by using the method of splitting into physical processes. This algorithm is called reversible reference system propagator algorithm (RESPA). It is also worth adding that with a variable integration step, even in the case of a pure Hamiltonian system, the constrained Hamiltonian will not be an integral and the boundedness of error in the deviation of the constrained Hamiltonian from the true one is not guaranteed [47]. To use symplectic methods effectively it is necessary to perform integration with a constant step. In the PHANTOM code, the time step is variable. In the general case with a variable step and taking into account dissipation it is possible to achieve convergence between the first and second order.

The total internal energy per unit mass is expressed by the equation

$$E = E_{\text{poly}} + E_{\text{therm}}, \tag{8}$$

where the energies of the polytropic part and ideal gas part per unit mass are written as

$$E_{\text{poly}} = K\frac{\rho^{\gamma-1}}{\gamma-1}, \tag{9}$$

$$E_{\text{therm}} = \frac{3}{2}\frac{\mathcal{R}T}{\mu}. \tag{10}$$

Since it is common for all SPH particles that $E_{\text{poly}} \gg E_{\text{therm}}$, the direct numerical solution of (7) leads to an erroneous estimate of temperature. We employed a different approach. Instead of (7), the equation for temperature is directly solved:

$$\frac{3}{2}\frac{\mathcal{R}}{\mu}\frac{\mathrm{d}T}{\mathrm{d}t} = -\frac{\mathcal{R}T}{\mu}(\nabla\cdot\mathbf{v}) + \Lambda_{\text{shock}}. \tag{11}$$

Determining the temperature numerically from Eq. (11), finding E_{poly} analytically from Eq. (9), and using (10) and (8), we obtain the desired total internal energy.

We now consider the following formulation of the problem. We take two polytropes with $n = 1$ (adiabatic exponent of matter $\gamma = 2$), which model two stars with masses $M_1 = 1.4M_\odot$ and $M_2 = 0.5M_\odot$ and identical radii $R_1 = R_2 = 10$ km. In the PHANTOM code, all SPH particles are taken to have identical masses. We used 10^5 SPH particles for the star M_1 and $3.5 \cdot 10^4$ SPH particles for the star M_2. The flow will start at a distance between the components of the binary system (see Eq. (3)) $a_{\text{c}} = R_2/f(q) \approx 34$ km. Naturally, one should remember the approximate nature of this expression derived in the limit of two point bodies. Assume that the distance a_0 between the components is 30 km. We place them in circular Kepler orbits and simulate in PHANTOM taking into account the correction (11) for the energy equation. The result is shown in Fig. 3.

The panels of the figure represent projections of what is happening onto the x, y plane (top view) for four moments of time t. It is seen that this is a typical merging process, preceded by the tidal disruption of a low-mass companion.

But what happens if at the initial moment the components are spaced further apart?

Our numerical experiments have shown that if we start with $a_0 = 36$ km, then the result will be a stable flow of matter (see Fig. 4). This plot shows only two moments in time, corresponding to the beginning and end of the simulation. It can be seen that stripping continues steadily for 20 revolutions (i. e., four times longer than the simulation in Fig. 3). We stopped the simulation because on such long times, numerous effects that are missing in our simple model should already be taken into account. First of all, these are the energy loss of the system due to gravitational radiation and a more realistic equation of state of the stars.

However, our goal has been achieved: a significant dependence of simulation results on the initial data has been demonstrated. In this regard, our conclusions coincide with the conclusions of the important paper [48], which considered the problem of correctly describing the fate of the white dwarfs binaries.

In addition, the stable flow regime we demonstrated numerically even in the case of polytropic equations of state contradicts the pessimistic conclusion of [16] and inspires some confidence.

We have also numerically studied the cases with other, not such extreme mass ratios in the NS binary system, namely, $M_1 = 2.0M_\odot$ and $M_2 = 1.0M_\odot$. The existence of a stable mass exchange regime has also been demonstrated for them with a distance $a_0 = 33$ km between the components.

However, moving to a detailed analysis of calculations on longer times should be done with caution due to the problem detected in the PHANTOM code.

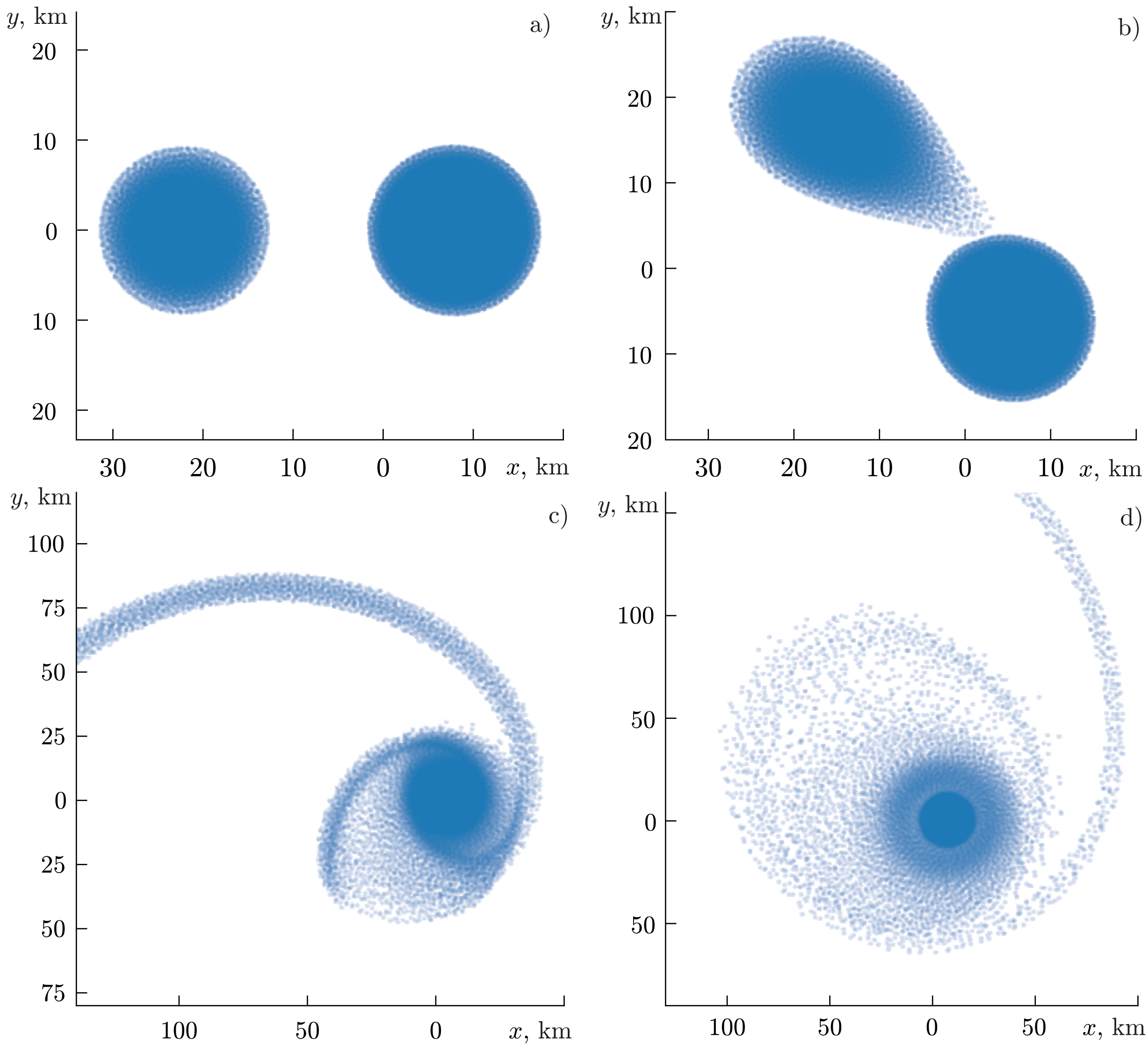

Fig. 3. Merging of two stars with $M_1 = 1.4M_\odot$ and $M_2 = 0.5M_\odot$ for time instants $t = 0.0$ ms (a), 0.3 ms (b), 5.5 ms (c), and 13.7 ms (d). Initial distance between the components is 30 km.

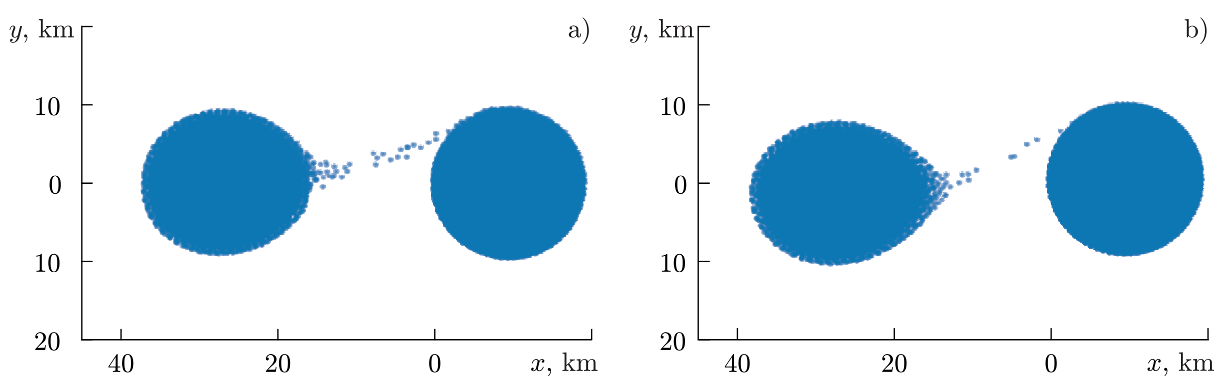

Fig. 4. Simulation of a binary system with the same parameters as in Fig. 3, but with $a_0 = 36$ km, at $t = 0$ (a) and $t = 20t_{\text{per}}$ (b).

4.2. Center of mass displacement

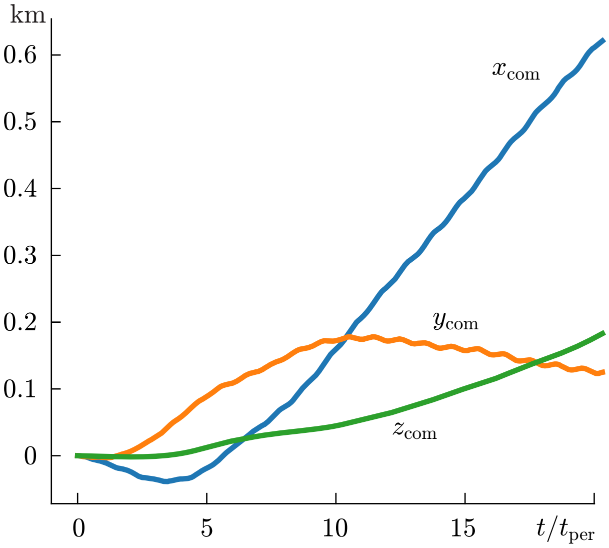

Fig. 5. Center of mass displacement for the same system as in Fig. 4.

As a result of working with the PHANTOM code, we detected an inherent error, namely, the center of mass displacement. Figure 5 shows the coordinates of the center of mass as functions of time for the system given in Fig. 4. We observed the same problem even when solving the relaxation problem for an individual NS. The center of mass of an NS with a mass of $0.5M_{\odot}$, consisting of $3.5 \cdot 10^4$ SPH particles, over long periods of time (about $10^4 u_{\text{time}}$), comparable to the duration of 20 revolutions of the systems considered above, shifts by a distance of about 1 km in the relaxation process!

The error is due to the incorrect allowance for self-gravity forces in PHANTOM. Solution of the Poisson equation $\nabla^2\Phi = 4\pi G\rho(\mathbf{r})$ for gravity in PHANTOM is obtained by dividing the total acceleration $\mathbf{a}_{\text{selfgrav}} = -\nabla\Phi$ into two parts, short- and long-range acceleration:

$$\mathbf{a}^p_{\text{selfgrav}} = \mathbf{a}^p_{\text{short}} + \mathbf{a}^p_{\text{long}}.$$

Above, Φ is the gravitational potential, ρ is the matter density calculated via SPH, and p is the index of the SPH particle. This division is dictated by considerations of speeding up calculations.

Short-range acceleration $\mathbf{a}^p_{\text{short}}$ is calculated by direct summation over the neighbor particles. To calculate the long-range acceleration components $\mathbf{a}^p_{\text{long}}$, the following procedure is used. All particles are hierarchically grouped into cells of the k-d tree. A tree leaf contains a maximum of 10 SPH particles. The components of gravitational acceleration of a particular chosen cell n, due to the attraction of all cells m, are obtained by multipole expansion of acceleration in powers of $1/r^2$:

$$a^i_n = \sum_m \left[-\frac{GM_m}{r^3} r^i + \frac{1}{r^4} \left(\hat{r}^k Q^m_{ik} - \frac{5}{2} \hat{r}^i \hat{r}^k \hat{r}^j Q^m_{jk} \right) \right].$$

Here, r^i is the ith component of the vector of the distance between the cells n and m, $\hat{r}^i$ is the corresponding ith component of the unit vector, M_m is the total mass of the cell m, and Q^m_{ik} is the component of the quadrupole moment of the cell m. The components of the gravitational acceleration of a specific SPH particle a in the chosen cell n are obtained by expanding a^i_n into a Taylor series to the second order:

$$a^i_{\text{long},p} = a^i_n + \Delta x^j \frac{\partial a^i_n}{\partial r^j} + \frac{1}{2} \Delta x^j \Delta x^k \frac{\partial^2 a^i_n}{\partial r^j \partial r^k},$$

where Δx^j is the relative distance of the particle p to the center of the cell n. This approach in PHANTOM is presented as a significant advantage compared to methods where multipole expansion is performed for each particle, skipping the Taylor expansion (see, e. g., [49]). However, it contains a key error. It can be shown that a non-physical uncompensated force arises, acting on each particle, while the total force f_{com} acting on the center of mass of the system will behave as

$$f_{\text{com}} \propto \frac{1}{h^2} \propto n_{\text{p}}^{2/3},$$

where h is the average dimensionless smoothing length of SPH and n_{p} is the average concentration of SPH particles. Increasing the number of particles for a more accurate description of density profiles, we simultaneously increase the imbalance of non-physical self-gravity.

During the calculation, such a random uncompensated force will act on the system as a whole at each counting step, shifting its center of mass from the initial position. The system ceases to be conservative, and we lose one of the main advantages of the SPH approach compared to the grid approach.

We are currently working to resolve this issue. The corresponding changes are being made to the PHANTOM code, and publication is being prepared.

5. DISCUSSION

Since the stripping model has received much less attention than the merging model, many of its aspects require further development. In this section, we will try to list and briefly discuss what remains to be done to ensure that the predictions of the stripping model have a reliable basis.

The first problem (which, by the way, is common for both models), is that of the true equation of state of a NS. Many predicted parameters of the model indirectly depend on this, in particular, the stripping time $t_{\rm str}$. For our model, an additional complexity is that the region of low NS masses ($M \lesssim M_\odot$), the description of which, as a rule, does not attract the attention of theorists (see, however, [50]), is also important here.

The second problem has already been discussed above when describing the modeling in PHANTOM. This is the sensitivity of the results obtained to the initial data. The problem, in fact, is divided into two parts. The first is that the initial configurations of the stars should be well relaxed in any case [37, 48]. If unperturbed stellar configurations are placed in the orbit at the initial moment of time, this can lead to various phenomena (oscillations, etc.) that are absent in reality and distort the simulation results. The second part of the problem concerns the correct accounting of losses due to gravitational radiation. As a rule, the impact of these losses is taken into account very approximately. For example, in PHANTOM the reaction force of gravitational wave radiation acting on each SPH particle is considered the same within one star [43], while in some models such a force is completely neglected [51].

For a strongly nonlinear stage of merging, lasting, as a rule, no more than several revolutions, such an approach can be justified, but for the stripping stage this is not at all the case. Actually, it is exactly losses due to gravitational radiation that determine the rate of the mass exchange process. Numerical accounting of these losses in a complex, dynamic binary system of non-point bodies with variable masses is a serious challenge to researchers.

The next important aspect of the mass exchange process in the stripping mechanism was identified as a result of our numerical experiments in PHANTOM, described in [29]. Mass exchange in a binary NS system leads to a significant spin-up of the massive companion. Thus, part of the orbital angular momentum is converted into its own spin M_1. Our preliminary calculations show that this effect can lead to a drastic reduction of the stripping time $t_{\rm str}$ and should be taken into account, in particular, for correct comparison with observational data (see also Figs. 1 and 2).

At the end of this section, we present a far from complete list of questions, requiring detailed study within the framework of the stripping mechanism. First, this is the fate of a massive NS (M_1) that increases its mass as a result of mass exchange. Does it remain a neutron star with rapid rotation, does it accelerate to critical rotation due to the spin-up effect discussed above, after which matter starts to flow out, or does it collapse into a black hole? And how do these processes affect, in fact, the stripping procedure itself? Related questions are as follows. What happens to the accreting material? What is the luminosity during accretion? Does an accretion disk form and, if so, can a jet of matter form?

Processes occurring in the low-mass component M_2 may also be important. While filling its Roche lobe, it is subject to tidal heating due to interactions in the binary system. Its matter also experiences a smooth decompression due to a decrease in its density, which can lead to additional heating. A low-mass neutron star has a specific structure [22], namely, a small core and an extended shell. Even relatively weak heating of this shell can greatly affect its structure, and hence the rate of mass transfer. In addition, the structure of the "hot" star M_2 when it reaches the minimum mass $M_{\rm min}$ may differ from the cold case, which will lead to a difference in the parameters of its explosion, and therefore, in those of the accompanying GRB as well.

Another important aspect still missing in the stripping model is comparison with optical observations of the kilonova at2017gfo [52]. From general considerations, it is clear that the explosion of a low-mass NS and the accompanying explosive decompression of approximately $M_{\min} \sim 0.1M_{\odot}$ of strongly neutronized matter should be accompanied by significant radiation powered by the radioactive decay of the elements generated in the explosion. It will be extremely interesting to find out whether the stripping scenario has any characteristic differences from merging in this aspect as well. We plan to perform the corresponding modeling in the near future. This modeling should be facilitated by the fact that, thanks to the geometry of the explosion of a low-mass NS, we can do it using the author's spherically symmetric code stella [53–56].

6. CONCLUSIONS

The presented review of the stripping model contains a discussion of many, although not all of its aspects. This model experienced a revival after a joint discovery of the gravitational wave signal GW170817 and the accompanying gamma-ray burst GRB170817A. Many of its parameters still need clarification and development. An extremely topical issue, for example, is the margin between merging/stripping scenarios. The answer to this question will determine the share of the stripping mechanism in the general population of short gamma-ray bursts. It should be emphasized that, in our opinion, both scenarios are not in an either/or antagonistic relationship. Rather, they complement each other: some conditions are good for merging and other conditions, for stripping.

Predictions of the stripping mechanism are quite certain: this is low energy, close to the spherical geometry of the explosion, and so on [22]. This compares favorably with the merging mechanism, within which there is a lot of uncertainties and adjustable parameters: by varying the direction of a jet, its opening angle [57], structure [58], parameters of the surrounding substance (cocoon, a choked jet [59]), and so on, one can explain any observational data. The stripping model is free of such arbitrariness. Of course, in both mechanisms there is a significant number of ambiguities, such as an unknown equation of state of superdense matter, complexity and inevitable simplifications in three-dimensional modeling of hydrodynamic phenomena in the general theory of relativity, and so on.

Even if the share of the stripping mechanism in the general GRB population is small, its influence can be significant in some respects. It should be remembered that the mass of ejected matter here is, in order of magnitude, equal to the minimum NS mass $M_{\min} \sim 0.1M_{\odot}$, which is high (see, e. g., [52]). Preliminary calculations of nucleosynthesis [60,61], accompanying the M_2 explosion look very promising, which, combined with the large amount of ejected mass, gives a hope for a large contribution of the stripping mechanism to the cosmic process of the formation of heavy elements.

S. I. Blinnikov, N. I. Kramarev and M. Sh. Potashov thank the Russian Science Foundation for support of simulations for modeling the mass exchange process in a close binary neutron star system using the smoothed particle hydrodynamics method (project No. 19-12-0229P). The authors thank the anonymous reviewer for a large number of valuable comments that contributed to the improvement of this work.

REFERENCES

1. J. Hjorth, J. Sollerman, P. Møller, et al., *Nature*, **423**, No. 6942, 847–850 (2003). https://doi.org/10.1038/nature01750
2. K. Nomoto, M. Tanaka, N. Tominaga, et al. https://arxiv.org/abs/0707.2219
3. S. E. Woosley. https://arxiv.org/abs/1105.4193
4. Y. W. Yu, J. P. Zhu, S. Z. Li, et al., *Astrophys. J.*, **840**, No. 1, 12 (2017). https://doi.org/10.3847/1538-4357/aa6c27
5. A. Suzuki, K. Maeda, and T. Shigeyama, *Astrophys. J.*, **870**, No. 1, 38 (2019). https://doi.org/10.3847/1538-4357/aaef85

6. J. M. Lattimer and D. N. Schramm, *Astrophys. J. Lett.*, **192**, L145–L147 (1974). https://doi.org/10.1086/181612
7. J. M. Lattimer and D. N. Schramm, *Astrophys. J.*, **210**, 549–567 (1976). https://doi.org/10.1086/154860
8. J. P. A. Clark and D. M. Eardley, *Astrophys. J.*, **215**, 311–322 (1977). https://doi.org/10.1086/155360
9. S. Bernuzzi, M. Breschi, B. Daszuta, et al., *Mon. Not. R. Astron. Soc.*, **497**, No. 2, 1488–1507 (2020). https://doi.org/10.1093/mnras/staa1860
10. L. Baiotti and L. Rezzolla, *Rep. Prog. Phys.*, **80**, No. 9, 096901 (2017). https://doi.org/10.1088/1361-6633/aa67bb
11. P. Haensel, A. Y. Potekhin, and D. G. Yakovlev, *Neutron Stars 1. Equation of State and Structure*, Springer, New York (2007).
12. S. I. Blinnikov, I. D. Novikov, T. V. Perevodchikova, and A. G. Polnarev, *Sov. Astron. Lett.*, **10**, 177–179 (1984).
13. S. I. Blinnikov, V. S. Imshennik, D. K. Nadezhin, et al., *Sov. Astron.*, **34**, 595–601 (1990).
14. A. V. Yudin, *Astron. Lett.*, **48**, 311–4320 (2022). https://doi.org/10.1134/S106377372206007X
15. K. V. Manukovskii, *Astron. Lett.*, **36**, 191–203 (2010). https://doi.org/10.1134/S1063773710030047
16. D. Lai, F. A. Rasio, and S. L. Shapiro, *Astroph. J.*, **420**, 811–829 (1994). https://doi.org/10.1086/173606
17. B. P. Abbott, R. Abbott, T. D. Abbott, et al., *Astrophys. J. Lett.*, **848**, No. 2, L12 (2017). https://doi.org/10.3847/2041-8213/aa91c9
18. B. P. Abbott, R. Abbott, T. D. Abbott, et al., *Astrophys. J. Lett.*, **848**, No. 2, L13 (2017). https://doi.org/10.3847/2041-8213/aa920c
19. B. D. Metzger, *Living Rev. Relativ.*, **23**, No. 1, 1 (2019). https://doi.org/10.1007/s41114-019-0024-0
20. A. Sneppen, D. Watson, A. Bauswein, et al., *Nature*, **614**, No. 7948, 436–439 (2023). https://doi.org/10.1038/s41586-022-05616-x
21. D. Dobie, D. L. Kaplan, T. Murphy, et al., *Astrophys. J. Lett.*, **858**, No. 2, L15 (2018). https://doi.org/10.3847/2041-8213/aac105
22. S. I. Blinnikov, D. K. Nadezhin, N. I. Kramarev, and A. V. Yudin, *Astron. Rep.*, **65**, 385–391 (2021). https://doi.org/10.1134/S1063772921050012
23. P. Jaranowski and A. Krolak, *Astrophys. J.*, **394**, 586–591 (1992). https://doi.org/10.1086/171610
24. L. D. Landau and E. M. Lifshitz, *Course of Theoretical Physics, Vol. 2, The Classical Theory of Fields*, Pergamon Press, 3rd English edition (1971).
25. T. M. Koshut, S. Kouveliotou, W. S. Paciesas, et al., *Astrophys. J.*, **452**, 145–155 (1995). https://doi.org/10.1086/176286
26. J. M. Pearson, N. Chamel, A. Y. Potekhin, et al., *Mon. Not. R. Astron. Soc.*, **481**, No. 3, 2994–3026 (2018). https://doi.org/10.1093/mnras/sty2413
27. G. Raaijmakers, S. K. Greif, T. E. Riley, et al., *Astrophys. J. Lett.*, **893**, No. 1, L21 (2020). https://doi.org/10.3847/2041-8213/ab822f
28. B. P. Abbott, R. Abbott, T. D. Abbott, et al., *Phys. Rev. X*, **9**, No. 1, 011001 (2019). https://doi.org/10.1103/PhysRevX.9.011001
29. S. I. Blinnikov, A. Yudin, N. Kramarev, and M. Potashov, *Particles*, **5**, 198–209 (2022). https://doi.org/10.3390/particles5020018

30. N. Kramarev and A. Yudin, *Mon. Not. R. Astron. Soc.*, **522**, No. 1, 626–634 (2023). https://doi.org/10.1093/mnras/stad1018

31. A. V. Yudin, T. L. Razinkova, and S. I. Blinnikov, *Astron. Lett.*, **45**, 847–854 (2019). https://doi.org/10.1134/S1063773719120077

32. Z. Kopal, *Close Binary Systems*, John Wiley & Sons, Hoboken (1959).

33. P. P. Eggleton, *Astrophys. J.*, **268**, 368–369 (1983). https://doi.org/10.1086/160960

34. B. Paczyński, *Acta Astron.*, **17**, 287–296 (1967).

35. K. C. B. New and J. E. Tohline, *Astrophys. J.*, **490**, 311–327 (1997). https://doi.org/10.1086/304861

36. P. M. Motl, J. Frank, J. Staff, et al., *Astrophys. J. Suppl. Ser.*, **229**, 27 (2017). https://doi.org/10.3847/1538-4365/aa5bde

37. J. A. Faber and F. A. Rasio, *Phys. Rev. D*, **62**, No. 6, 064012 (2000). https://doi.org/10.1103/PhysRevD.62.064012

38. J. A. Faber, F. A. Rasio, and J. B. Manor, *Phys. Rev. D*, **63**, 044012 (2001). https://doi.org/10.1103/PhysRevD.63.044012

39. J. A. Faber and F. A. Rasio, *Phys. Rev. D*, **65**, 084042 (2002). https://doi.org/10.1103/PhysRevD.65.084042

40. T. Dietrich, M. Ujevic, W. Tichy, et al., *Phys. Rev. D*, **95**, No. 2, 024029 (2017). https://doi.org/10.1103/PhysRevD.95.024029

41. D. Radice, A. Perego, J. Hotokezaka, et al., *Astrophys. J.*, **869**, No. 2, 130 (2018). https://doi.org/10.3847/1538-4357/aaf054

42. L. Baiotti, *Arab. J. Math.*, **11**, 105–118 (2022). https://doi.org/10.1007/s40065-021-00357-7

43. D. J. Price, J. Wurster, T. S. Tricco, et al., *Publ. Astron. Soc. Aust.*, **35**, e031 (2018). https://doi.org/10.1017/pasa.2018.25

44. J. Monaghan, *J. Comput. Phys.*, **82**, 1–15 (1989). https://doi.org/10.1016/0021-9991(89)90032-6

45. O. P. Stoyanovslaya and V. N. Snytnikov, *Matem. Model.*, **22**, No. 5, 29–44 (2010).

46. S. I. Blinnikov, N. V. Dunina-Barkovskaya, and D. K. Nadyozhin, *Astrophys. J. Suppl. Ser.*, **106**, 171–203 (1996). https://doi.org/10.1086/192334

47. V. A. Avdyushev, *Numerical Modeling of Orbits* [in Russian], Nauchno-Tekhnicheskaya Literatura, Tomsk (2010).

48. M. Dan, S. Rosswog, J. Guillochon, and E. Ramirez-Ruiz, *Astrophys. J.*, **737**, No. 2, 89 (2011). https://doi.org/10.1088/0004-637X/737/2/89

49. W. Dehnen, *Astrophys. J.*, **536**, No. 1, L39–L42 (2000). https://doi.org/10.1086/312724

50. H. O. Silva, H. Sotani, and E. Berti, *Mon. Not. R. Astron. Soc.*, **459**, No. 4, 4378–4388 (2016). https://doi.org/10.1093/mnras/stw969

51. M. Toscani, G. Lodato, D. J. Price, and D. Liptai, *Mon. Not. R. Astron. Soc.*, **510**, No. 1, 992–1001 (2022). https://doi.org/10.1093/mnras/stab3384

52. D. M. Siegel, *Eur. Phys. J. A*, **55**, No. 11, 203 (2019). https://doi.org/10.1140/epja/i2019-12888-9

53. S. I. Blinnikov, F. K. Röpke, E. I. Sorokina,, et al., *Astron. Astrophys*, **453**, No. 1, 229–240 (2006). https://doi.org/10.1051/0004-6361:20054594

54. S. I. Blinnikov, E. G. Eastman, O. S. Bartunov, et al., *Astrophys. J.*, **496**, No. 1, 454–472 (1998). https://doi.org/10.1086/305375

55. S. I. Blinnikov, P. Lundqvist, O. S. Bartunov, et al., *Astrophys. J.*, **532**, No. 2, 1132–1149 (2000). https://doi.org/10.1086/308588
56. S. I. Blinikov, "Nonstationary radiative and hydrodynamic processes in supernova stars" [in Russian], D. Sc. theses, Moscow (2000).
57. D. Finstad, S. De, D. A. Brown, et al., *Astrophys. J. Lett.*, **860**, No. 1, L2 (2018). https://doi.org/10.3847/2041-8213/aac6c1
58. D. Lazzati, D. López-Cámara, M. Cantiello, et al., *Astrophys. J. Lett.*, **848**, No. 1, L6 (2017). https://doi.org/10.3847/2041-8213/aa8f3d
59. O. Gottlieb, E. Nakar, T, Piran, and K. Hotokezaka, *Mon. Not. R. Astron. Soc.*, **479**, No. 1, 588–600 (2018). https://doi.org/10.1093/mnras/sty1462
60. I. V. Panov and A. V. Yudin, *Astron. Lett.*, **46**, 518–527 (2020). https://doi.org/10.1134/S1063773720080034
61. C. M. Yip, M. C. Chu, S. C. Leung, and L. M. Lin. https://arxiv.org/abs/2211.14023